Propose of Design Method on Level II load of open Sabo dam

Toshiyuki Horiguchi[1*], *Satoshi* Katsuki[2], *and Yoshiharu* Komatsu[1]

[1] National Defence Academy Engineering Department, 2380018 Yokosuka Kanagawa, Japan
[2] Emeritus Professor, National Defence Academy Engineering Department, 2380018 Yokosuka Kanagawa, Japan

Abstract. This study presents a load model of the Level II design for a steel pipe open Sabo dam. The Level II design is associated with a lower occurrence frequency than the conventional design concept, to the performance of debris flow trapping efficacy against higher discharge caused by heavy precipitation in recent years. A dynamic load model reveals experimental observations, and static models similar to the conventional design load models are evaluated from the viewpoint of a rational load. Dynamic and elastoplastic analyses are conducted for one structure, and three types of basin area models utilized Level II load models using a dynamic load. The safety evaluation results confirm that the design load models are composed of each other.

1 Introduction

In recent year, steel pipe open Sabo dams have been constructed to maintain continuity river for environment. However, there have been reports of damage by the generation of debris flows that exceed the design load [1]. Therefore, a system for a design load level larger than the current design load level (hereafter, Level-II) is studied [2,3]. Ishikawa et al. [3] proposed that a Level-II load can be set under excess probability (200-1000 years). Ishikawa [4] proposed a method for probabilistically estimating the planned peak debris flow by indicating the correlation between the amount of sediment and basin area. However, the definition of combining Level-II loads and structural responses remains unclear.

The study proposes a method for setting the Level-II load in the design of open Sabo dams, and examines the Level-II verification method which assumes that the limit state of the structural response is the limit value of the elasto-plastic response of the member. In addition, a static design load equivalent to the dynamic design one is examined.

2. Proposed Level-I load and Level-II load

The proposed design loads can be considered based on the form of the current design load in Fig.1. For Model-I as Level-I load, the debris flow fluid force statically acts on the upper part, and the sediment pressure load statically acts on the lower part. The debris flow load is determined from the rainfall of 100 year excess probability. The stability of the structure is an allowable stress design method that ensures that each member is within the elastic response value. Model-II is a dynamic load proposed by Komatsu et al. [5]. Because Model II make the structural response a dynamic response, it is possible to reproduce close to the actual situation. If the limit state in the design is defined as the plastic rotation angle of the member reaching the allowable rotation angle, the verification is expressed below.

$$\delta_{i\text{-}max} \le \delta_{ai} \left(=\frac{\delta_{fi}}{\gamma_D}\right) \tag{1}$$

where, $\delta_{i\text{-}max}$ is the maximum deformation of the member, δ_{ai} is the allowable deformation of the member, δ_{fi} is the failure deformation of the member, γ_D is the safety factor corresponding to the dynamic response.

The fracture deformation of a member is limit state. The safety factors corresponding to the dynamic response are those for Level II loads. This study utilizes the 99 % prediction line illustrated in Fig. 2.

The design of the open Sabo dam is based on data obtained from topographic surveys. The amount of sediment released is determined by comparing the amount of sediment that can be moved within the basin area, with the amount of sediment that can be transported by a planned debris flow based on the amount of rainfall. The peak flow can be expressed by the following equation:

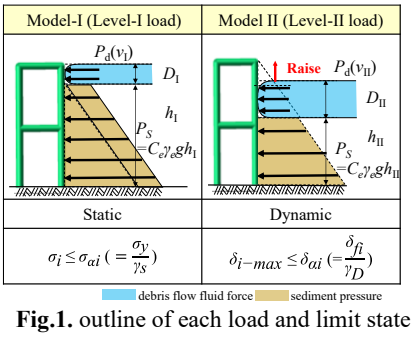

Fig.1. outline of each load and limit state

* Corresponding author: htoshi@nda.ac.jp

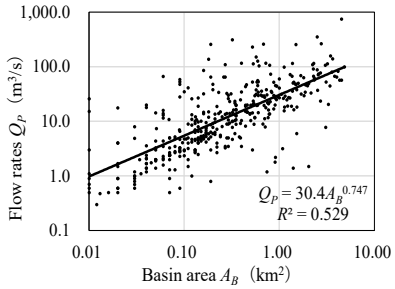

(a) Level-I load

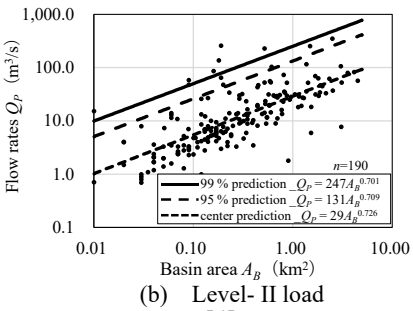

(b) Level- II load

Fig. 2. Flow rates-basin area relationship [4]

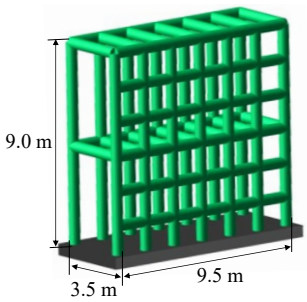

Fig.3. Open sabo dam model

$$Q_P = 0.01 \cdot \frac{C_* \times V_{dqp}}{C_d} \quad (2)$$

where Q_P is the peak flow rate (m³/s), C_* is the volumetric concentration of deposited sediment, V_{dqp} is the sediment volume (m³), C_d is the flow rate is planned at the installation location.

The flow rate is initially planned at the installation location. The flow rate is obtained using the regression equation illustrated in **Fig. 2(a)** [4].

$$Q_{P\,\mathrm{I}} = 30.4\, A_B^{0.747} \quad (3)$$

where $Q_{P\,\mathrm{I}}$ is the flow rate of the Level-I load (m³/s), *AB is* the basin area (km²).

The velocity of the debris flow is determined using Manning's equation as follows:

$$v = \left(\frac{1}{n}\right) \cdot D_r^{2/3} \cdot (\sin\theta_s)^{1/2} \quad (4)$$

where v is the velocity of the debris flow (m/s), n is Manning's roughness coefficient (s・m$^{-1/3}$) (n = 0.1 used in the design), D_r is the diameter depth (m) ($D_r \approx D_d$ (: water depth (m)), and θ_S is the slope of the stream bed.

The equation of continuity is expressed as follows:

$$Q = A_d \cdot v \quad (5)$$

where Q is the flow rate (m³/s), A_d is the cross-sectional area (m²). The cross-sectional area of the flow can be expressed by the following equation:

$$A_d = D_d \cdot B_{da} \quad (6)$$

where B_{da} is the width of flow (m).

The 99 % prediction line can be used to establish the planned sediment discharge and flow rate for Level-II load shown to Fig. 2(b) [4].

$$Q_{P\,\mathrm{II}} = 247.0\, A_B^{0.701} \quad (7)$$

where, $Q_{P\,\mathrm{II}}$ is the flow rate (m³/s) of the Level-II load.

The debris flow fluid force is expressed below.

$$F = K_h \cdot \frac{\gamma_d}{g} \cdot D_d \cdot v^2 \quad (8)$$

where F is the debris flow force (kN/m), K_h is the coefficient of debris flow force, γ_d is the unit volume weight of the debris flow (15.8 kN/m³), g is the gravitational acceleration. Sediment pressure acts below the depth of the debris flow from the height of the dam.

$$P_{eH} = \frac{1}{2} \cdot C_e \cdot \gamma_e \cdot h_e^2 + C_e \cdot \gamma_e \cdot D_d \cdot h_e \quad (9)$$

where P_{eH} is the sediment pressure (kN/m), C_e is the earth pressure coefficient (0.45), γ_e is the unit volume weight of the sediment (15.3 kN/m³), h_e is the sediment height (m).

The time required for the debris flow to reach the top of the open Sabo dam is defined.

$$t_H = \frac{0.5 \cdot H^2}{v \cdot D_d \cdot \tan\theta_r} \quad (10)$$

where, t_H is the time (s) for the debris flow to reach the front of open Sabo dam, H is the open Sabo dam height (m), θ_r is the angle of repose upstream of the open-type Sabo dam (θ_r = 35 ° was used).

3 Examination condition

3.1 Basin condition

Basin area is adopted as a parameter in the analysis. Three cases of basin area A_B = 0.5, 1.0, 2.0 km² are adopted. The bed slope is set as the slope of the debris flow section (θ_s = 10 °). The design condition is a riverbed width of B_{da} = 10.7 m.

3.2 Open Sabo dam model

As shown to Fig. 3, an open Sabo dam model is 9.0 m height, 9.5 m width, and 3.5 m depth. All the joints are of the same cross-section, and joint pipes are not considered in open Sabo dam model. The spacing between each member is set with a maximum gravel diameter 1.0 m. The cross section of the steel pipe is set to a diameter D = 508 mm, wall thickness t = 22 mm. The open Sabo dam model for the basin area is assumed under the same conditions. The steel pipe material used is STK490. The compression and tension are set to the same value for computational efficiency. Bending failure is considered instead of failure. The sectioning method is employed to obtain the bending moment-curvature relationship, axial force-strain relationship, and torsional moment–torsional rate relationship for a circular tube cross-section. FEM is utilized for this analysis, which is capable of simulating large

Table 1. Setting condition of level-I load

Basin area A_B (km^2)	0.5	1	2
Flow rate Q_{P1} (m^3/s)	18.1	30.4	51.0
Flow velocity U_{d1} (m^2/s)	2.9	3.6	4.4
Depth D_{d1} (m)	0.6	0.8	1.1
Debris flow load F_1 (N/m^2)	1.68×10^4	2.61×10^4	3.93×10^4
Sediment pressure P_{eH} (N/m^2)	3.43×10^4	3.55×10^4	3.72×10^4

Table 2. Setting condition of level- II load

Basin area A_B (km^2)	0.5	1	2
Flow rate $Q_{P\,II}$ (m^3/s)	151.9	247.0	401.5
Flow velocity U_d (m^2/s)	6.8	8.3	10.0
Depth D_d (m)	2.1	2.8	3.7
Debris flow load F (N/m^2)	9.48×10^4	1.40×10^5	2.10×10^5
Time to reach top	4.07 s	2.5 s	1.57 s

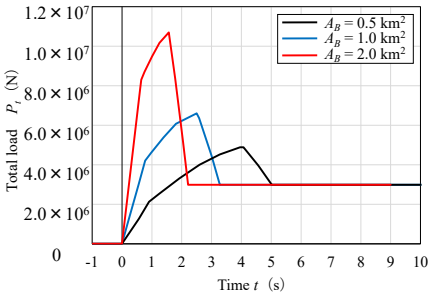

Fig. 4. Load-time relationship

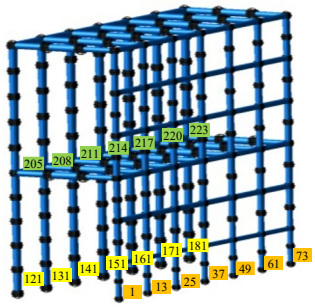

Fig. 5. Each member

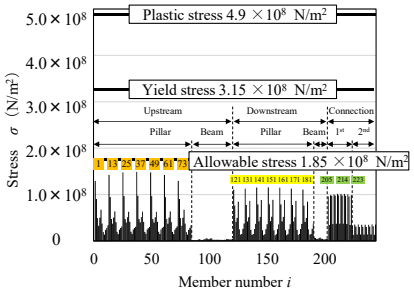

Fig. 6. Stresses in members at level-I load of Model-I (A_B = 2.0 km^2)

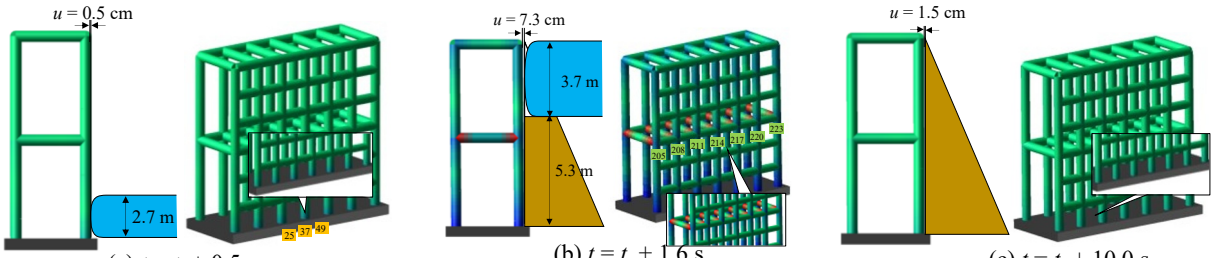

(a) $t = t_0 + 0.5$ s (b) $t = t_0 + 1.6$ s (c) $t = t_0 + 10.0$ s

Fig. 7. Structural response of Model-II (A_B = 2.0 km^2)

deformations of structures. The amount of plastic deformation is determined using the associated flow law.

The limit value of the plastic rotation angle is set to the limit corresponding to the local buckling during compression. In addition, the function Φ_y representing the elastic limit and plasticization function are expressed by the following equations:

$$\Phi_y = \left(\frac{M_1}{M_y}\right)^2 + \left(\frac{M_2}{M_y}\right)^2 + \left(\frac{N}{N_y}\right)^2 + \left(\frac{T}{T_y}\right)^2 - 1.0 \le 0 \quad (11)$$

$$\Phi_P = \left(\frac{M_1}{M_P}\right)^2 + \left(\frac{M_2}{M_P}\right)^2 + \left(\frac{N}{N_P}\right)^2 + \left(\frac{T}{T_P}\right)^2 - 1.0 \le 0 \quad (12)$$

where M_1 is the bending moment around the cross-sectional principal axis, M_2 is the bending moment around the cross-sectional axis, N is the axial force, T is the torsional moment, M_Y is the yield moment, M_P is the plastic moment, N_Y is the yield axial force, N_P is the plastic axial force, T_Y is the yield torsional moment, and T_P is the plastic torsional moment.

3.3 Level-I load

Table 1 presents the parameters for Level-I load. Eqs (4)-(7), (9), (10) are adopted to determine the debris flow load and sediment pressure in each basin area. The structural response of the structure is investigated by static analysis under the influence of debris flow forces and sediment pressure. The Level-I load is ‘static load’.

3.4 Level-II load

Table 2 present the parameters for Level-II load. Eqs (5)-(11) are adopted to determine the debris flow forces and time to reach the top of the open Sabo dam for each basin area. The load-time relationship acting on each node is illustrated in **Fig.4**. The maximum total load for a basin area of A_B = 0.5 km^2 is 57.1 kN/m^2. The maximum total load for a basin area of A_B = 1.0 km^2 is 77.2 kN/m^2. The maximum total load for a basin area of A_B = 2.0 km^2 is 128.7 kN/m^2. The load reduction after the maximum total load decreased is similar to the slope at which the maximum load is reached. This is a dynamic loading model that remains constant when the sediment pressure load is reached. The Level-I load is ‘dynamic load’.

4 Analytical results and discussion

4.1 Level-I load

The analysis resulted in an elastic response. Fig.5 illustrates the locations of the members. Fig.6 illustrates the stresses in the members by basin area. Stresses in the members are indicated at the top, and stresses in the upstream and downstream column members and first-stage joint are indicated. The stresses are expressed using the following equations:

$$\sigma_i = \frac{M_{max}}{Z} + \frac{N}{A_m} \quad (13)$$

where, σ_i is the stress in member i (N/m^2), M_{max} is the maximum bending moment in the cross section (N·m), Z is the section modulus (m^3), N is the axial force (N), A_m *is* the cross-sectional area of the member (m^2).

4.2 Model-II

Fig.7 shows the simulated structural response of Model II (A_B = 2.0 km^2). Fig.7(a) illustrates that the height reaches 2.7 m above the bottom of the open Sabo dam.

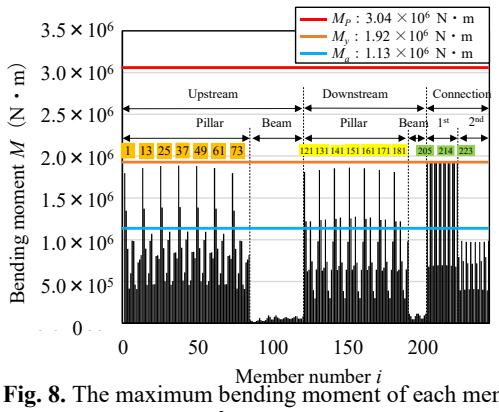

Fig. 8. The maximum bending moment of each member in A_B = 2.0 km² (Model-II)

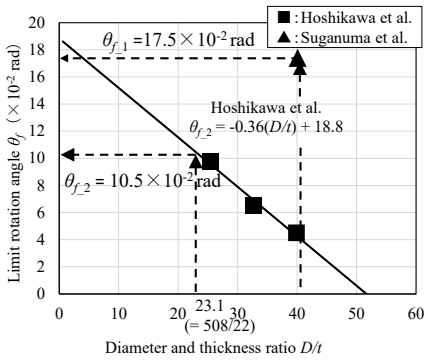

Fig.9. Limit rotation angle to diameter and thickness ratio relationship

Members 25, 37, and 49 are the allowable stress limits. The horizontal displacement at the top of the open Sabo dam is u = 0.5 cm. Fig.7(b) illustrates that when the load reaches the top of the open-type Sabo dam, the total load reaches its maximum value F_{max} = 1.07×10⁴ kN. The upstream and downstream ends of the first horizontal joint are in an elastoplastic region ($\Phi_y \leq \Phi \leq \Phi_P$), resulting in a horizontal displacement *of* u = 7.3 cm at the top of the open-type Sabo dam. Fig. 7(c) illustrates the end of the debris flow force action and sediment pressure load acting on the front of the open Sabo dam. All members are elastic, and the horizontal displacement at the top of the open Sabo dam is u = 1.5 cm.

Fig. 8 illustrates the maximum bending moment of each member in Model II. The bending moments of all members are indicated at the top, and the bending moments of the upstream and downstream column members and first-stage joint members are indicated at the bottom. A large bending moment occurs in the first-stage horizontal joint material. The maximum bending moment for each member in the basin area A_B = 2.0 km² is M_{max} = 1.93×106 N・m for member 214. Bending moments close to the yield bending moment occur in the upstream and downstream column members and in the first-stage horizontal joint. In particular, the first-stage horizontal joint material is plasticized.

Fig. 9 illustrates a study of the limit rotation angle due to the local buckling of the steel pipes. Suganuma et al. [7] illustrated a bending moment and rotation angle relationship for a diameter-to-thickness ratio D/t = 40.1. The angle of rotation corresponding to the maximum bending moment is θ_{f_1} = 17.5 × 10⁻² rad (≈ 10 °). Hoshikawa et al. [8] proposed the following equation for the critical rotation angle θ_{f_2}, which corresponds to local buckling:

$$\theta_{f\_1} = 17.5\times10^{-2} \text{ rad} \quad (15)$$

$$\theta_{f\_2} = -0.36\cdot(D/t)+18.8 \quad (16)$$

Substituting D/t = 23.1 for this analytical model into this equation, we obtain θ_{f_2} = 10.5 × 10⁻² rad (≈ 6 °). The ratios of the respective plastic rotation angles are approximately 30 and 18, respectively. Therefore, the following description is based on the most stressed basin area A_B = 2.0 km².

5. Conclusions

The results are summarized as follows:

(1) Level-II loads were considered assuming a 99 % non-exceedance probability.

(2) The proposed design load models were Model-II for dynamic analysis of structural response. The characteristics of each design load model were evaluated by numerical analysis on a typical structural model.

(3) In Model-II, the dynamic effect was negligible, and the plastic rotation angle generated in the member was evaluated to be approximately 1/20 of the rotation angle limit value, which is sufficient to provide a safety margin.

This study evaluated the response from structural stability based on the worst load, and the effects of actual sediment/soils need to be investigated.

References

1. Hiramatsu S.et al., *Mudslide disaster in Nagiso town, Nagano Prefecture on July 9, 2014*, JSECE, Vol.67, No.3, pp.38-48 (2014)
2. Sonoda Y.et al., *A fundamental study on the load carrying capacity of steel frame check dam*, *JSCE*, Vol.62A, pp.1019-1030 (2016)
3. Ishikawa N.et al., *A study on necessity and setting method of large-scale debris flow (Level II load)*, proceedings of Sabo conference, Vol.67, pp.57-58 (2018)
4. Ishikawa Y., *Estimation of runoff sediment volume and peak discharge of debris flow based on a stochastic method and effects of drainage basin area, precipitation and geology on them*, JSECE, Vol.73, No.5, pp. 15-26 (2021)
5. Komatsu Y. et al., *Experimental study on debris flow impact load against overturning limit of steel open type Sabo dam*, *JSCE*,Vol.67A, pp.838-848 (2021)
6. Sabo, Landslide Technical Center, *Steel Erosion Control Structures Design Handbook* (2010)
7. Suganuma J. and Kono J., *Bending capacity of locally deformed line pipes*, Journal of Structural Engineering, Vol. 65A, pp. 236-249 (2019)
8. Hoshikawa T. et al., *A Study on Dynamic Ultimate Limit of Steel Pipe Open Sabo Dam*, *JSCE*, Vol. 525, I-33, pp. 139-152 (1995)